

Reversal of the Intramolecular Charge Transfer in *p*-Dimethylaminobenzanilides by Amido Anilino Substitution

Xuan Zhang,[†] Chao-Jie Wang,[‡] Li-Hong Liu,[†] and Yun-Bao Jiang^{*,†}

Department of Chemistry and the MOE Key Laboratory of Analytical Sciences, Xiamen University, Xiamen 361005, China, and Department of Chemistry and the State Key Laboratory for Physical Chemistry of Solid Surfaces, Xiamen University, Xiamen 361005, China

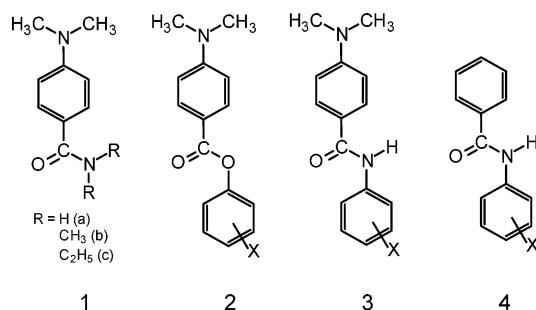
Received: June 24, 2002; In Final Form: September 25, 2002

p-Dimethylaminobenzanilides with a para or meta substituent at the amido anilino moiety were designed to generate a series of dual fluorescent molecules of variable electron acceptors. Ab initio calculations indicated that the anilino substitution did not lead to an obvious change in the ground-state structures of the fluorophores, and the ¹H NMR signal of the amido –NH proton was found to experience a linear downfield shift with increasing σ of the substituent, supporting the fact that the amido anilino moiety was indeed varied comparably by the substitution. The intramolecular charge transfer dual fluorescence was indeed observed in solvents over a large polarity range from the nonpolar cyclohexane (CHX) through diethyl ether (DEE) and tetrahydrofuran (THF) to highly polar acetonitrile (ACN). It was found that the CT emission shifted to the blue with increasing electron-withdrawing ability of the amido anilino substituent up to a Hammett constant σ of ca. +0.39 and to the red at higher σ . The solvent polarity variation did not change the σ value at which the CT emission shift direction reverses. Similar variation profiles were also observed with the CT to LE emission intensity ratio and the total fluorescence quantum yield. It was concluded that the CT direction in *p*-dimethylaminobenzanilides was reversed by the amido anilino substitution, and the CT occurs from amido anilino to benzoyl moiety at low σ , whereas at high σ , the CT switches to that from dimethylamino to the benzanilide moiety, which was also supported from the Hartree–Fock calculations. This finding provides an alternative method based on substituent effect for identifying the charge-transfer direction in multiple charge-transfer systems. The results suggested that the anilino group could be a much stronger electron donor than an aliphatic amino group, which would be of use in designing electron donor substituted molecules. In both cases the dependences of the CT emission energy against σ of the substituent at the amido aniline phenyl ring were found to be much stronger than that in the ester counterparts of *p*-dimethylaminobenzanilides. This interesting σ dependence in the CT emission would be of significance in developing new fluorescent sensors based on electron donor/acceptor variations in *p*-dimethylaminobenzanilides.

1. Introduction

For understanding of the intramolecular charge transfer (CT) photophysics of the DMABN-like dual fluorescent electron donor/acceptor para-substituted benzenes, investigations of the influence of the electron donor and/or acceptor have been an important strategy.^{1–8} It has been shown that, although a comparable variation in the dialkylamino electron donor group by changing alkyl substituents is successful, with the electron acceptor, replacing the cyano group with other electron-withdrawn groups such as an ester and amide is not feasible because of the accompanied change in the CT photophysics, e.g., DMABN versus its ester derivative,^{2,6} and the steric effect.⁸ Rettig et al.⁸ have designed a series of *p*-dimethylaminobenzamides (**1**, Scheme 1) attempting to decrease the electron-accepting ability of the acceptor by changing the amide group from –C(O)NH₂ through –C(O)N(CH₃)₂ to –C(O)N(C₂H₅)₂. Accordingly, they indeed observed a systematic blue shift of

SCHEME 1: Molecular Structures of *p*-Dimethylaminobenzamides (1**), Phenyl *p*-Dimethylaminobenzoates (**2**), *p*-Dimethylaminobenzanilides (**3**), and Benzanilides (**4**)^a**



^a Substituents in **3** are *p*-CH₃ (**a**), *m*-CH₃ (**b**), H (**c**), *p*-F (**d**), *p*-Cl (**e**), *m*-Cl (**f**), *m*-Br (**g**), *p*-CO₂CH₃ (**h**), *p*-COCH₃ (**i**), and *p*-NO₂ (**j**), and those in **4** are *p*-OCH₃ (**a**), *p*-CH₃ (**b**), H (**c**), *p*-F (**d**), *p*-Cl (**e**), *p*-CO₂CH₃ (**f**), *p*-COCH₃ (**g**), and *p*-NO₂ (**h**), respectively.

the CT emission and the decrease in the CT to LE intensity ratio. Meanwhile, the accompanied steric contribution due to the alkyl substitutions in the amide moiety that influenced the conjugation of the amide moiety with the phenyl ring made it difficult to abstract the real electronic polar effect. We have

* To whom correspondence should be addressed. Phone/Fax: +86 592 2185662. E-mail: ybjiang@xmu.edu.cn.

[†] Department of Chemistry and the MOE Key Laboratory of Analytical Sciences, Xiamen University.

[‡] Department of Chemistry and the State Key Laboratory for Physical Chemistry of Solid Surfaces, Xiamen University.

chosen an alternative way by designing phenyl *p*-dimethylaminobenzoates (**2**, Scheme 1) hoping to comparably vary the electron acceptor by introducing a substituent at the ester phenyl ring thereby avoiding the possible steric effect. Indeed, we showed that the substituent did not affect the ground-state structure of the ester and observed that the CT emission energy varied linearly with the Hammett constant of the substituent.⁹ In that case, however, the substituent tuning efficiency was not high with the Hammett linear slope value lower than 0.2. A possible reason could be the lower conjugation extent between the phenoxy oxygen atom with its phenyl ring as suggested by a high dihedral angle of around 50°. In benzanilide, the conjugation extent of the anilino nitrogen atom with the phenyl ring could be much higher because a nearly planar structure was shown for the aniline moiety.¹⁰ It was therefore expected that in the amide counterparts of phenyl *p*-dimethylaminobenzoates, *p*-dimethylaminobenzanilides (**3**, Scheme 1), the amido phenyl substituent might have a higher efficiency in influencing the CT behavior if similar CT photophysics applies to these two kinds of molecules.

With *p*-dimethylaminobenzanilides, however, an additional CT reaction channel might exist as that with benzanilides (**4**, X = H and other para substituents, Scheme 1), in which the CT occurs from the anilino donor to the benzoyl acceptor.^{10–15} The CT state of benzanilide (**4**) has also been suggested to be of the twisted configuration^{10,12,15} as is done with *p*-dimethylaminobenzamides. In particular, the CT emission could even be seen in a nonpolar solvent,^{10–15} which might suggest a low activation energy of the CT process in **4**. Therefore, with **3**, there could be two competitive charge-transfer processes.

Results with *p*-dimethylaminobenzamides (**1**) showed that, with increasing electron donating strength of the amido moiety, from $-\text{NH}_2$ through $-\text{N}(\text{CH}_3)_2$ to $-\text{N}(\text{C}_2\text{H}_5)_2$, which leads to the decrease in the electron accepting ability of the benzamide acceptor, the CT emission shifted to the blue together with a decrease in the CT to LE intensity ratio, whereas the CT direction remained unchanged as from the dimethylamino donor to the benzamide acceptor.⁸ Similar charge transfer was also assigned in a secondary amide derivative of **1** ($-\text{C}(\text{O})-\text{NHCH}_2\text{C}_5\text{H}_5\text{N}^{16}$) that has an amide moiety sterically similar to **1a**. Electrochemically, the anilino group is a stronger electron donor than the diethylamino group according to the oxidation potentials of aniline ($E_{\text{ox}} = 0.96 \text{ V}$) and diethylamine ($E_{\text{ox}} = 1.31 \text{ V}$).¹⁷ This suggests the possibility, but does not necessarily mean, that the charge transfer with *p*-dimethylaminobenzanilides (**3**) would be that which occurs with benzanilides (**4**, Scheme 1) from the amido anilino moiety to the dimethylaminobenzoyl moiety, with the direction of the charge transfer with **3**, hence, remaining to be investigated.

In the present paper, we will show that, with the synthesized series of *p*-dimethylaminobenzanilides (**3**, Scheme 1) with a substituent at the amido anilino moiety ranging from electron donating to withdrawing, the CT is not unidirectional. We found that, although the electron density at the amido nitrogen atom indeed experienced a monotonic decrease with increasing electron withdrawing ability of the substituent, the CT emission shifted initially to the blue and then to the red when the substituent was highly electron accepting. This observation clearly indicated that the CT direction with **3** was reversed by amido anilino substitution.

2. Experimental Section

2.1. Experimental Techniques. Corrected fluorescence spectra were recorded on a Hitachi F-4500 fluorescence spectrophotometer using excitation and emission slits of 5 nm. The

excitation wavelength was 305 nm. Fluorescence quantum yields were measured using quinine sulfate as the standard (0.546 in 0.5 mol L⁻¹ H₂SO₄¹⁸). The absorption spectra were taken on a Beckman DU-7400B or Varian Cary 300 absorption spectrophotometer using a 1 cm quartz cell. IR spectra were taken on a Nicolet FT-IR 360 with a KBr pellet, and ¹H NMR data were acquired in DMSO-*d*₆ on a Varian Unity⁺ 500 MHz NMR spectrometer using TMS as an internal reference.

All ab initio calculations were performed on a DELL PC using the Gaussian 98 suit of programs.^{19a} Ground-state structures were fully optimized at the Hartree–Fock (HF) self-consistent field level. The internally stored pseudopotentials and LANL1DZ basis sets were used to all sorts of atoms in *p*-dimethylaminobenzanilides (**3**, Scheme 1). The singlet excited-state energies were calculated by means of the time-dependent Hartree–Fock (TDHF)^{19b} method on HF optimized ground-state structures.

2.2. Materials. *p*-Aminobenzoic acid and substituted anilines were purchased from Shanghai Chemical Reagents Company, China National Chemicals Group (Shanghai, China) and used for synthesis without further purification. *p*-Dimethylaminobenzoic acid was prepared from the reaction of *p*-aminobenzoic acid with dimethyl sulfate.²⁰ Anilino-substituted benzanilides (**4**, Scheme 1) were synthesized by procedures described previously.¹⁵ Solvents for spectroscopic investigations were purified before use and checked to have no fluorescent impurity at the used excitation wavelength. All spectra were measured at a sample concentration of ca. 10⁻⁵ mol L⁻¹.

2.3. General Procedures for the Synthesis of *p*-Dimethylaminobenzanilides (3**).** *p*-Dimethylaminobenzoic acid and the corresponding substituted aniline were heated to melt or to reflux in acetonitrile and to which POCl₃ was dropped. After about 0.5 h, the residue was cooled to room temperature and washed with dilute aqueous NaOH, and a yellow precipitate was collected by filtration and was washed alternatively by dilute HCl and NaOH. The crude products were subject to repeated recrystallizations from acetone to give the desired compounds in 50–80% overall yield based on *p*-dimethylaminobenzoic acid.

4-Dimethylamino-4'-methylbenzanilide (**3a**). IR (KBr, cm⁻¹): 3354, 3037, 2921, 1639, 1606. ¹H NMR (500 MHz, DMSO-*d*₆): δ (ppm) 2.265 (s, 3H), 2.996 (s, 6H), 6.751 (d, 2H, $J = 9 \text{ Hz}$), 7.116 (d, 2H, $J = 8 \text{ Hz}$), 7.635 (d, 2H, $J = 8.5 \text{ Hz}$), 7.850 (d, 2H, $J = 9 \text{ Hz}$), 9.776 (s, 1H).

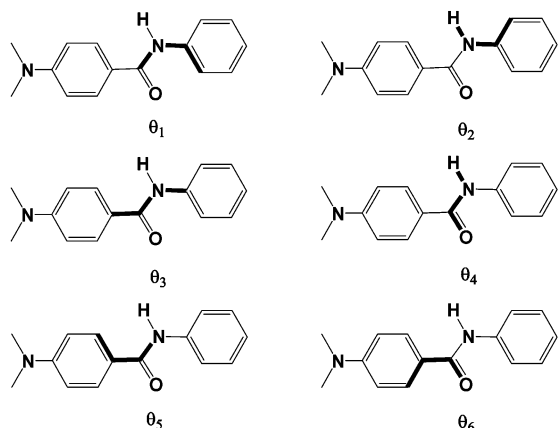
4-Dimethylamino-3'-methylbenzanilide (**3b**). IR (KBr, cm⁻¹): 3327, 3041, 2921, 1644, 1610. ¹H NMR (500 MHz, DMSO-*d*₆): δ (ppm) 2.295 (s, 3H), 2.999 (s, 6H), 6.756 (d, 2H, $J = 8.5 \text{ Hz}$), 6.866 (d, 1H, $J = 7 \text{ Hz}$), 7.190 (t, 1H, $J = 8 \text{ Hz}$), 7.553 (d, 1H, $J = 8 \text{ Hz}$), 7.602 (s, 1H), 7.857 (d, 2H, $J = 9 \text{ Hz}$), 9.774 (s, 1H).

4-Dimethylaminobenzanilide (**3c**). IR (KBr, cm⁻¹): 3315, 3038, 2916, 1634, 1604. ¹H NMR (500 MHz, DMSO-*d*₆): δ (ppm) 3.003 (s, 6H), 6.761 (d, 2H, $J = 8.5 \text{ Hz}$), 7.045 (t, 1H, $J = 7.5 \text{ Hz}$), 7.314 (t, 2H, $J = 8 \text{ Hz}$), 7.760 (d, 2H, $J = 8.5 \text{ Hz}$), 7.864 (d, 2H, $J = 9 \text{ Hz}$), 9.859 (s, 1H).

4-Dimethylamino-4'-fluorobenzanilide (**3d**). IR (KBr, cm⁻¹): 3334, 3062, 2825, 1650, 1608. ¹H NMR (500 MHz, DMSO-*d*₆): δ (ppm) 3.000 (s, 6H), 6.759 (d, 2H, $J = 9 \text{ Hz}$), 7.156 (t, 2H, $J = 9 \text{ Hz}$), 7.757–7.785 (m, 2H), 7.855 (d, 2H, $J = 8.5 \text{ Hz}$), 9.916 (s, 1H).

4-Dimethylamino-4'-chlorobenzanilide (**3e**). IR (KBr, cm⁻¹): 3344, 3093, 2923, 1653, 1608. ¹H NMR (500 MHz, DMSO-*d*₆): δ (ppm) 3.003 (s, 6H), 6.760 (d, 2H, $J = 9 \text{ Hz}$), 7.370 (d, 2H, $J = 9 \text{ Hz}$), 7.805 (d, 2H, $J = 9 \text{ Hz}$), 7.855 (d, 2H, $J = 9 \text{ Hz}$), 9.985 (s, 1H).

SCHEME 2: Selected Dihedral Angles



4-Dimethylamino-3'-chlorobenzanilide (**3f**). IR (KBr, cm^{-1}): 3322, 3060, 2893, 1645, 1612. ^1H NMR (500 MHz, $\text{DMSO}-d_6$): δ (ppm) 3.007 (s, 6H), 6.767 (d, 2H, $J = 8.5$ Hz), 7.098 (d, $J = 8.5$ Hz, 1H), 7.344 (t, 1H, $J = 8.5$ Hz), 7.699 (d, 1H, $J = 8$ Hz), 7.860 (d, 2H, $J = 9$ Hz), 7.971 (s, 1H), 10.012 (s, 1H).

4-Dimethylamino-3'-bromobenzanilide (**3g**). IR (KBr, cm^{-1}): 3321, 3070, 2892, 1644, 1610. ^1H NMR (500 MHz, $\text{DMSO}-d_6$): δ (ppm) 3.006 (s, 6H), 6.765 (d, 2H, $J = 9$ Hz), 7.230 (d, 1H, $J = 8$ Hz), 7.284 (t, 1H, $J = 8$ Hz), 7.749 (d, 1H, $J = 7.5$ Hz), 7.858 (d, 2H, $J = 8.5$ Hz), 8.105 (s, 1H), 9.998 (s, 1H).

4-Dimethylamino-4'-methoxycarbonylbenzanilide (**3h**). IR (KBr, cm^{-1}): 3336, 3078, 2946, 1710, 1654, 1608. ^1H NMR (500 MHz, $\text{DMSO}-d_6$): δ (ppm) 3.012 (s, 6H), 3.830 (s, 3H), 6.772 (d, 2H, $J = 9.5$ Hz), 7.882 (d, 2H, $J = 9$ Hz), 7.933 (s, 4H), 10.181 (s, 1H).

4-Dimethylamino-4'-methylcarbonylbenzanilide (**3i**). IR (KBr, cm^{-1}): 3340, 3093, 2921, 1665, 1654, 1605. ^1H NMR (500 MHz, $\text{DMSO}-d_6$): δ (ppm) 2.539 (s, 3H), 3.013 (s, 6H), 6.774 (d, 2H, $J = 8.5$ Hz), 7.889 (d, 2H, $J = 9$ Hz), 7.939 (s, 4H), 10.172 (s, 1H).

4-Dimethylamino-4'-nitrobenzanilide (**3j**). IR (KBr, cm^{-1}): 3401, 3087, 2910, 1651, 1604. ^1H NMR (500 MHz, $\text{DMSO}-d_6$): δ (ppm) 3.021 (s, 6H), 6.784 (d, 2H, $J = 8.5$ Hz), 7.899 (d, 2H, $J = 8.5$ Hz), 8.058 (d, 2H, $J = 9$ Hz), 8.239 (d, 2H, $J = 9$ Hz), 10.432 (s, 1H).

3. Results and Discussion

3.1. Ground-State Structures of *p*-Dimethylaminobenzanilides (3**).** In *p*-dimethylaminobenzanilides (**3a–3j**, Scheme 1), the substituent was introduced in the amido anilino phenyl ring at the para or meta position but not at the ortho position to avoid the possible steric effect. To confirm that no substantial steric effect was introduced by the substitution, the ground-state structures of **3** were optimized by the ab initio method. The calculations indicated that **3c** in the trans conformation was lower for ca. 3.8 kcal mol $^{-1}$ in energy than that in the cis conformation at Hartree–Fock (HF) level which included the zero-point energy correction. The following calculations were therefore only carried out on the trans amides. The calculated ground-state conformations of **3** were almost planar at the amido anilino moiety as seen from the dihedral angles θ_1 , θ_2 , θ_3 , and θ_4 (Scheme 2 and Table 1) and have large amide benzoyl dihedral angles around 20° (θ_5 and θ_6 , Scheme 2 and Table 1). It was seen from Table 1 that the amido anilino substitution did not lead to discernible changes in the dihedral angles (<2°) and bond lengths, revealing that the ground-state structures did

TABLE 1: Calculated Dihedral Angles and Bond Lengths of **3** in the Ground State^a

	dihedral angles, $^\circ$ ^b						bond lengths, Å			
	θ_1	θ_2	θ_3	θ_4	θ_5	θ_6	C(O)–N	C=O	Ph–N	Ph–C(O)
3a	1.3	2.5	176.7	172.3	20.2	17.5	1.370	1.234	1.420	1.490
3b	1.6	2.1	176.6	172.3	20.1	17.5	1.371	1.237	1.419	1.490
3c	1.3	2.3	176.7	172.3	20.1	17.4	1.372	1.237	1.419	1.489
3d	1.2	2.5	176.8	172.4	19.5	16.9	1.373	1.237	1.418	1.488
3e	0.8	2.6	176.7	172.6	18.7	16.2	1.374	1.236	1.416	1.487
3f	0.9	2.5	176.8	172.3	19.2	16.3	1.376	1.235	1.414	1.487
3g	1.2	2.3	176.8	172.5	19.2	16.5	1.375	1.236	1.415	1.487
3h	1.6	1.9	176.4	172.2	19.5	16.8	1.377	1.235	1.411	1.488
3i	1.8	1.8	176.5	172.2	19.4	16.7	1.377	1.235	1.411	1.487
3j	1.6	1.8	176.4	172.2	18.6	15.9	1.382	1.234	1.405	1.484

^a Molecular structures of **3** shown in Scheme 1. ^b Dihedral angles defined in Scheme 2.

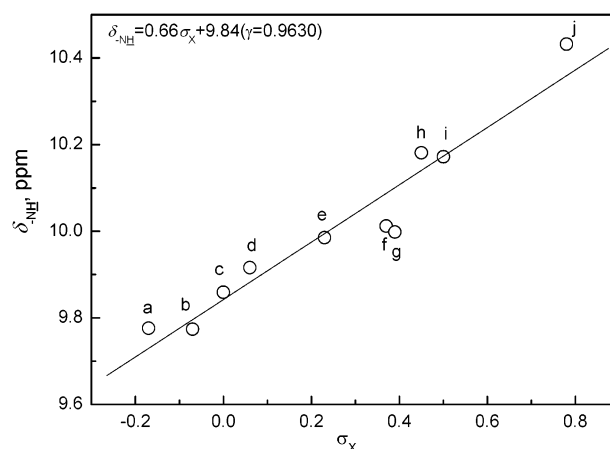


Figure 1. Linear dependence of the ^1H NMR chemical shift of the amido $-\text{NH}$ proton against the Hammett constant²¹ of the substituent at the amido aniline phenyl ring in *p*-dimethylaminobenzanilides. The substituents are (a) *p*- CH_3 , (b) *m*- CH_3 , (c) H, (d) *p*-F, (e) *p*-Cl, (f) *m*-Cl, (g) *m*-Br, (h) *p*- CO_2CH_3 , (i) *p*- COCH_3 , and (j) *p*- NO_2 , respectively. The NMR spectra were taken in $\text{DMSO}-d_6$ using tetramethylsilicate (TMS) as internal standard.

not undergo obvious variation within the substitution series. This means that the substituent effect, if any, would originate from the substituent electron polar effect.

The ^1H NMR signals of the amido $-\text{NH}$ protons were monitored and correlated to the Hammett substituent constant, σ .²¹ We observed that, with increasing electron-withdrawing ability of the substituent, the ^1H NMR signal experienced a continuous downfield shift, which was indicated by a nice linear dependence of the chemical shift against σ with a slope of +0.66, Figure 1. This means that a monotonic decrease in the electron density at the amido $-\text{NH}$ nitrogen atom occurs with increasing electron-withdrawing ability of the substituent. Therefore, in case that the CT in **3** is identified as that in **1**, the electron acceptors in **3** are indeed varied comparably by the amido anilino substitution.

3.2. Absorption and Fluorescence Spectra. The absorption spectra of *p*-dimethylaminobenzanilides (**3**, Scheme 1) in cyclohexane (CHX), diethyl ether (DEE), tetrahydrofuran (THF), and acetonitrile (ACN) of increasing polarity were recorded and parts of the spectral parameters were summarized in Table 2. It was found from Table 2 that the absorption spectra of all of the 10 *p*-dimethylaminobenzanilide derivatives (**3a–3j**) had a main intense band peaked at 306–330 nm that slightly shifted to the red with increasing solvent polarity. The observed molar absorption coefficients at the order of magnitude of 10^4 mol $^{-1}$ L cm $^{-1}$ (Table 2) were indicative of the (π , π^*) transition

TABLE 2: Absorption and Fluorescence Spectral Data for 3 in Organic Solvents

X	solvent ^a	absorption ^b		fluorescence	
		λ_{\max} , nm	ϵ , 10 ⁴ L mol ⁻¹ cm ⁻¹	$\lambda_{LE}/\lambda_{CT}$, nm	Φ^d
3a <i>p</i> -CH ₃	CHX	306	2.15	340/465	0.0015
	DEE	307	3.39	345/518	0.0034
	THF	311	3.02	351/532	0.0028
	ACN	312	2.62	364/502	0.0027
3b <i>m</i> -CH ₃	CHX	306	2.56	340/452	0.0013
	DEE	306	3.35	342/498	0.0048
	THF	311	2.96	353/518	0.0044
	ACN	314	3.47	367/502	0.0063
3c H	CHX	307	3.52	338/448	0.0011
	DEE	307	4.06	344/494	0.0036
	THF	311	3.73	352/500	0.0061
	ACN	314	3.79	367/494	0.0107
3d <i>p</i> -F	CHX	307	2.74	340/452	0.0011
	DEE	307	3.50	345/500	0.0034
	THF	311	3.31	354/504	0.0053
	ACN	314	3.31	367/492	0.0104
3e <i>p</i> -Cl	CHX	309	3.91	338/435	0.0011
	DEE	310	4.23	346/481	0.0050
	THF	315	4.22	356/490	0.0101
	ACN	317	4.17	370/498	0.0171
3f <i>m</i> -Cl	CHX	310	3.08	338/-	0.0031
	DEE	311	3.60	348/445	0.0103
	THF	314	3.70	358/455	0.0263
	ACN	318	3.83	373/496	0.0319
3g <i>m</i> -Br	CHX	310	3.84	338/-	0.0033
	DEE	312	4.78	348/445	0.0108
	THF	317	4.52	358/455	0.0256
	ACN	318	4.42	373/496	0.0367
3h <i>p</i> -CO ₂ CH ₃	CHX	318	4.93	343/-	0.0148
	DEE	319	5.53	356/-	0.0512
	THF	324	5.27	386/470	0.1984
	ACN	326	5.65	370/516	0.0209
3i <i>p</i> -COCH ₃	CHX	321	3.07	~345 +/-	0.0006
	DEE	323	3.75	356/470	0.0010
	THF	328	3.97	368/468	0.0158
	ACN	331	3.75	378/550	0.0017
3j <i>p</i> -NO ₂	CHX	337 (278)	1.10 (0.42)	~360 +/-	<0.0001
	DEE	345 (283)	2.85 (1.18)	388/536	0.0006
	THF	353 (290)	2.60 (1.35)	400/-	0.0003
	ACN	354 (294)	2.46 (1.28)	430/-	0.0002

^a Solvent: CHX, cyclohexane; DEE, diethyl ether; THF, tetrahydrofuran; ACN, acetonitrile. ^b Parameters of the second absorption band are given in the parentheses. ^c Uncertainty due to poor solubility. ^d Fluorescence quantum yield.

character. Within the molecule series of **3a–3j**, the absorption spectrum maximum in each solvent was found to remain nearly constant for **3a–3d** and underwent a very slight red-shift until **3g** with a substituent σ of +0.39, which was followed by a substantial red-shift at higher σ (Table 2). This is clearly indicated in Figure 2 in which the absorption maximum was plotted against the Hammett substituent constant. The substantial red-shift in the absorption maximum with increasing σ of higher than +0.39 suggests that a ground-state charge transfer toward the substituted amido anilino moiety in **3** might occur. At σ lower than +0.39, there was practically no ground-state charge transfer as the absorption maximum remained almost unchanged with amido anilino substitution.

The fluorescence spectra were therefore recorded. Indeed, as expected for the *p*-dimethylaminobenzamide derivatives (**1**, Scheme 1), dual fluorescence was observed for *p*-dimethylaminobenzanilides (**3**, Scheme 1) in most cases, see Table 2 and Figures 3 and 4. In Figure 3, it was shown as an example that, although the short-wavelength emission of **3a** underwent minor red-shift, the long-wavelength emission shifted dramatically to the red with increasing solvent polarity, pointing to the charge-

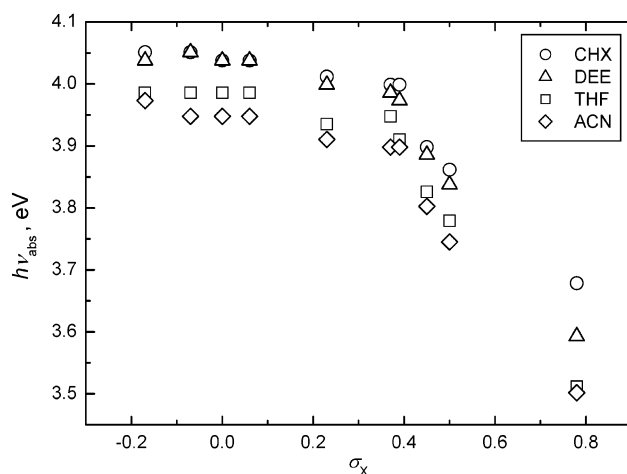


Figure 2. Plots of the absorption maximum of **3** against the Hammett constant of the substituent at the amido anilino phenyl ring. Solvent: CHX, cyclohexane; DEE, diethyl ether; THF, tetrahydrofuran; and ACN, acetonitrile.

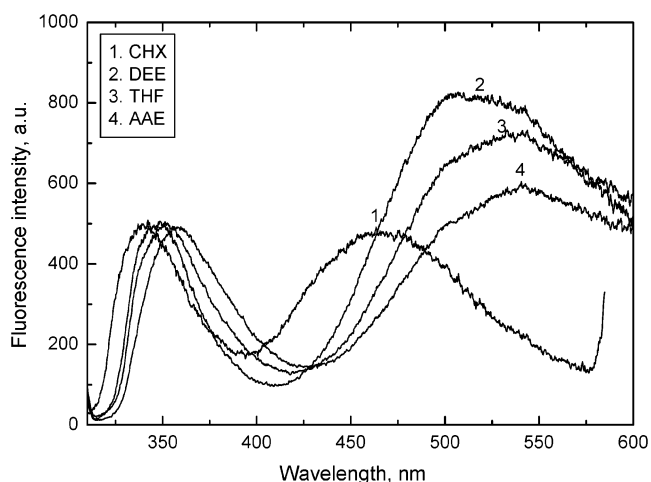


Figure 3. Normalized fluorescence spectra of **3a** in solvents of varied polarity. Solvent: CHX, cyclohexane; DEE, diethyl ether; THF, tetrahydrofuran; and AAE, ethyl acetate.

transfer character of the emissive state. The dual fluorescence was hence assigned to the LE and the CT states,^{1–3,8,9} respectively. It was found, however, that with part of the *p*-dimethylaminobenzanilides **3** dual fluorescence could be observed even in nonpolar solvent cyclohexane (Figure 4a), whereas with *p*-dimethylaminobenzamides, no such dual fluorescence but only the LE emission was shown in the nonpolar solvent,⁸ suggesting that the involved CT process with the former molecules would have a very low activation energy. Most strikingly, it was found in Figure 4 that the long-wavelength CT emission shifted to the blue when the amido moiety became increasingly electron-withdrawing as the substituent on the amido aniline became more electron demanding from *para*-methyl (**3a**) to *meta*-Cl (Br) (**3f** and **3g**), suggesting that the substituent is located at the electron donor moiety. With **3h–3j**, no CT-like long-wavelength emission was observed in the nonpolar solvent, whereas in polar solvents such as DEE and THF, the long-wavelength CT emission turned to shift to the red with increasing electron withdrawing ability of the substituent as expected in the cases of *p*-dimethylaminobenzamides **1**⁸ and in **2**, the ester counterparts of **3** (Scheme 1).⁹ In Figure 5, the CT emission energies were plotted against the Hammett substituent constants in which a clear turn was found at

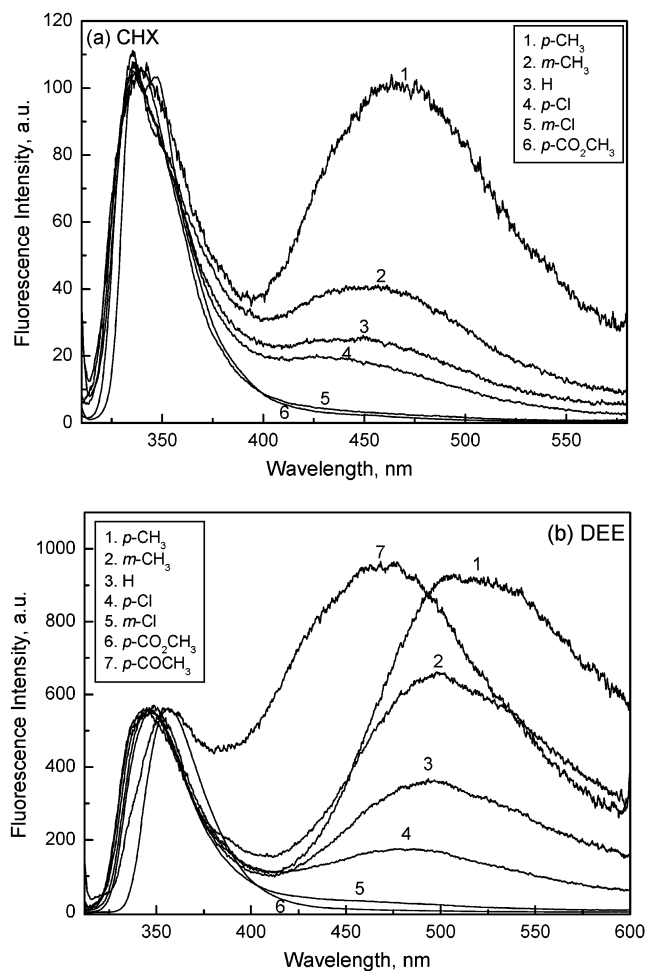


Figure 4. Normalized fluorescence spectra of **3** in (a) cyclohexane and (b) diethyl ether. The substituents in **3** are indicated in the inset.

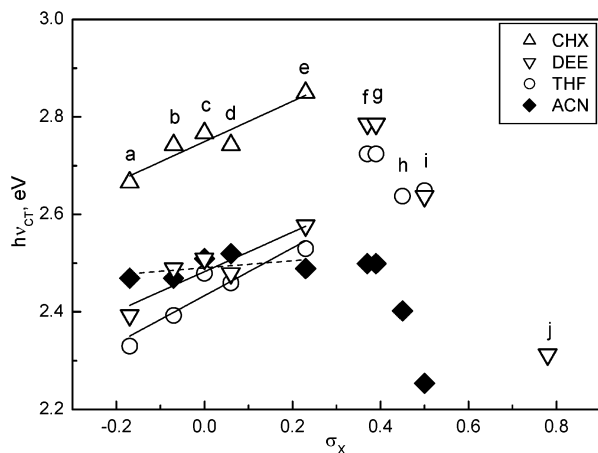


Figure 5. Plots of the CT emission energy versus the Hammett substituent constant.

σ of around +0.39. No such turn was found with benzanilides **4** without the dimethylamino group (Scheme 1) whose CT emission in CHX was found to shift to the blue with increasing electron-withdrawing ability of the substituent,^{15b} and a linear dependence was found between the CT emission energy and the Hammett substituent constant with a slope of +0.41 eV and an intercept of 2.46 ($\gamma = 0.9364$, $n = 7$). It was thus clear that at a σ of +0.39 the direction of charge transfer in *p*-dimethylaminobenzanilides **3** was reversed. At a σ lower than +0.39, the charge transfer with **3** was the benzanilide-like charge transfer from the aniline to benzoyl moiety,^{10–15} whereas at

TABLE 3: TDHF Calculated Singlet Excited-State Energy, Absorption Maximum Wavelength, Oscillator Strength, and Transition Compositions

		ΔE , eV ^a	$\lambda_{\text{calc.}}$, nm ^b	λ_{scaled} , nm ^c	f^d	$^n\chi_m(\%)^e$
3a	S ₁	5.3925	230	310	0.6660	⁰ $\chi_0(69)$
	S ₂	5.6361	220	297	0.0660	¹ $\chi_0(52)$, ⁰ $\chi_3(23)$, ¹ $\chi_1(21)$
	S ₃	5.8013	214	288	0.0485	² $\chi_1(36)$, ² $\chi_0(30)$, ³ $\chi_2(19)$
3b	S ₁	5.3996	230	310	0.6109	⁰ $\chi_0(73)$
	S ₂	5.6371	220	297	0.0586	¹ $\chi_0(62)$, ⁰ $\chi_3(23)$
	S ₃	5.8918	210	283	0.0499	² $\chi_2(30)$, ⁰ $\chi_1(26)$, ³ $\chi_1(21)$
3c	S ₁	5.3941	230	310	0.6177	⁰ $\chi_0(75)$
	S ₂	5.6364	220	297	0.0593	¹ $\chi_0(64)$, ⁰ $\chi_3(23)$
	S ₃	5.8941	210	283	0.0691	⁰ $\chi_1(26)$, ² $\chi_2(21)$, ³ $\chi_1(16)$
3d	S ₁	5.3823	230	310	0.6051	⁰ $\chi_0(78)$
	S ₂	5.6335	220	297	0.0542	² $\chi_0(69)$, ⁰ $\chi_2(14)$
	S ₃	5.8854	211	284	0.0492	¹ $\chi_1(63)$, ¹ $\chi_0(12)$
3e	S ₁	5.3646	231	311	0.6858	⁰ $\chi_0(79)$
	S ₂	5.6316	220	297	0.0564	² $\chi_0(65)$, ⁰ $\chi_3(22)$
	S ₃	5.8727	211	284	0.0467	¹ $\chi_1(53)$, ³ $\chi_2(17)$
3f	S ₁	5.3685	231	311	0.6434	⁰ $\chi_0(74)$
	S ₂	5.6327	220	297	0.0530	¹ $\chi_0(66)$, ⁰ $\chi_3(22)$
	S ₃	5.9119	210	283	0.0619	⁰ $\chi_5(28)$, ⁰ $\chi_1(22)$, ² $\chi_2(17)$
3g	S ₁	5.3696	231	311	0.6492	⁰ $\chi_0(76)$
	S ₂	5.6330	220	297	0.0540	² $\chi_0(43)$, ¹ $\chi_0(24)$, ⁰ $\chi_3(22)$
	S ₃	5.8828	211	284	0.0697	¹ $\chi_1(26)$, ⁰ $\chi_1(21)$, ³ $\chi_2(12)$
3h	S ₁	5.2859	235	317	0.9988	⁰ $\chi_0(50)$, ¹ $\chi_0(19)$
	S ₂	5.5707	223	301	0.0842	⁰ $\chi_1(43)$, ¹ $\chi_0(30)$
	S ₃	5.6451	220	297	0.0058	² $\chi_0(62)$, ¹ $\chi_3(15)$
3i	S ₁	4.6060	269	363	0.0001	⁰ $\chi_4(46)$, ¹ $\chi_4(22)$, ⁴ $\chi_4(22)$
	S ₂	5.2513	236	318	1.0075	⁰ $\chi_0(43)$, ⁰ $\chi_1(22)$, ¹ $\chi_0(16)$
	S ₃	5.5173	225	303	0.0286	⁰ $\chi_1(43)$, ¹ $\chi_0(35)$
3j	S ₁	4.2843	289	390	0.0000	⁰ $\chi_8(75)$, ² $\chi_8(16)$
	S ₂	4.6934	264	356	0.0005	⁰ $\chi_9(76)$, ⁴ $\chi_9(15)$
	S ₃	5.0842	244	329	1.0275	⁰ $\chi_1(58)$, ¹ $\chi_0(18)$, ⁰ $\chi_0(16)$

^a Singlet excited-state energy. ^b Singlet excited-state energy given in wavelength. ^c Scaled by a factor of 1.35. ^d Oscillator strength. ^e The percentage of a transition from the (HOMO - m)th orbital to the (LUMO + n)th orbital.

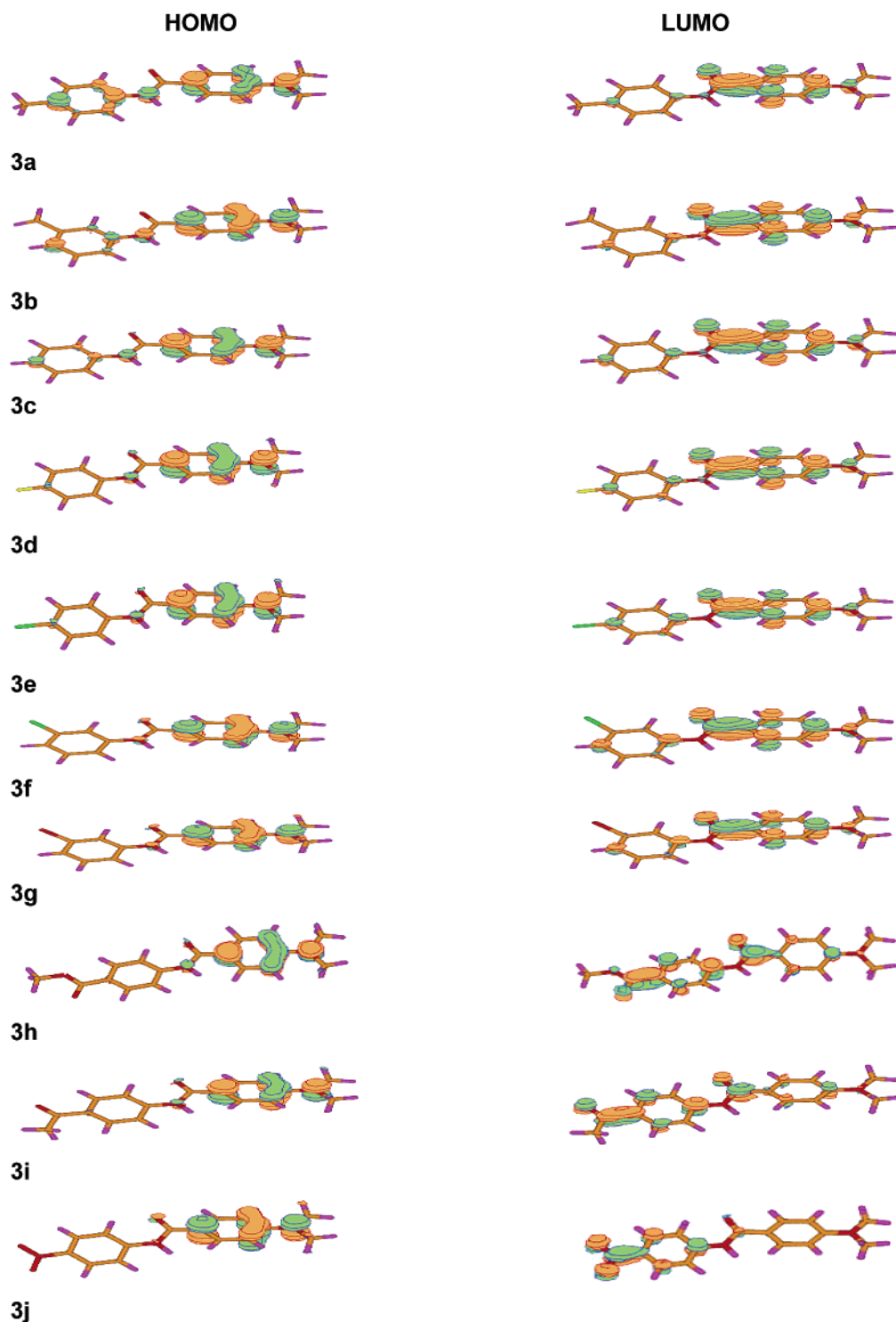
higher σ , it turns out to be the *p*-dimethylaminobenzamide-like charge transfer from dimethylamino group to the rest of the molecule as assumed for **1**.^{1,2,8} Therefore, the present finding on the substituent effect provides an alternative method in identifying the charge-transfer direction in a system where multiple charge-transfer possibilities exist. It is also of significance to note that the charge transfer in *p*-dimethylaminobenzanilides **3a–3e** even with an electron-withdrawing substituent at the amido anilino group (*p*-F and *p*-Cl in **3d** and **3e**, respectively) is not that which occurred in *p*-dimethylaminobenzamides (**1**), suggesting that the anilino group is indeed a stronger electron donor than the aliphatic amino groups. Similar observations were also made in several other systems,^{22–24} which would be of use in designing electron donor/acceptor substituted charge-transfer molecules.

3.3. Switching of the Intramolecular Charge Transfer.

Previously, we have shown that the charge-transfer emission energy, $h\nu^{\text{max}}(\text{CT})$, varied linearly with the Hammett constant of the substituent in the electron acceptor or donor of substituted-phenyl *p*-dimethylaminobenzoates⁹ and benzanilides,¹⁵ eq 1, provided that the singlet excited-state energy, $E_{0,0}$, and the ground-state repulsion energy, δE_{rep} , or their difference are constant within the molecule series. In eq 1, R and T are the gas constant and absolute temperature, respectively, and ρ is the reaction constant as defined in the classic Hammett linear free energy formula:

$$h\nu^{\text{max}}(\text{CT}) = -2.303RT\rho\sigma + E_{0,0} - \delta E_{\text{rep}} + \text{constant} \quad (1)$$

With **3** at a σ lower than +0.39, it was observed that the

SCHEME 3: MOLDEN²⁵ Plots of the HOMO and LUMO Orbitals of 3

absorption maximum and the LE emission energy (Table 2 and Figure 2) were nearly constant within the **3a–3e** series, suggesting that the singlet excited-state energy is almost constant. δE_{rep} could be reasonably assumed to be constant for **3a–3e** because of their similar structure. Equation 1 thus holds for **3a–3e**. We found from Figure 5 that in CHX, DEE, and THF, the linear slopes were 0.41, 0.40, and 0.49 eV, respectively, which are also close to that found for **4** in CHX (0.41 eV), indicating that the reaction constant ρ is practically independent of solvent polarity. This means that, with **3a–3e** in these solvents of increasing polarity, only the benzanilide-like CT reaction occurs, without the contribution of the other,

the *p*-dimethylaminobenzamide-like, CT reaction. In the highly polar solvent ACN, however, the corresponding linear slope of 0.07 eV is much lower. As in a more polar solvent, the charge transfer is enhanced, which would lead to a higher linear slope;¹⁵ the present observation of a much lower slope in ACN would mean that the benzanilide-like CT reaction in **3a–3e** is mixed with the *p*-dimethylaminobenzamide-like CT reaction, which was further supported by the fact that in several cases the CT emission in ACN was more blue-shifted than that in less polar solvent THF, because the *p*-dimethylaminobenzamide-like CT emission⁸ locates at a shorter wavelength than the benzanilide-like CT emission.¹⁵

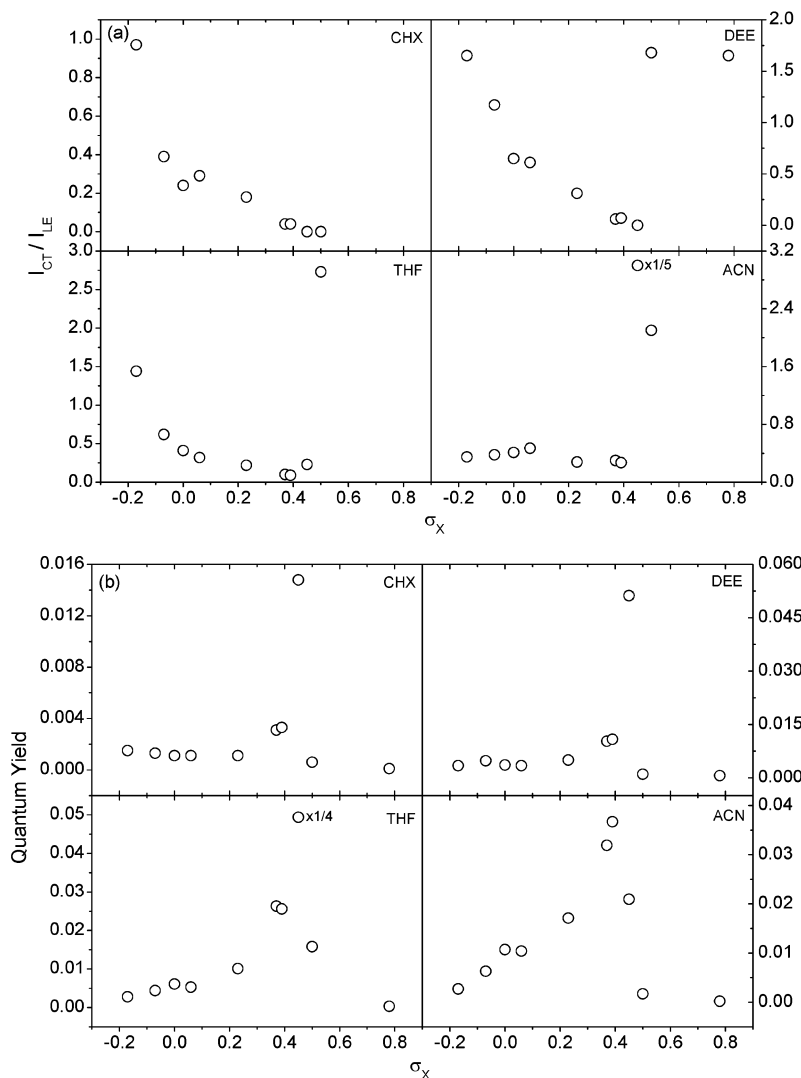


Figure 6. Variations of (a) the CT to LE emission intensity ratio and (b) the total fluorescence quantum yield with substituent constant.

With **3h–3j**, the *p*-dimethylaminobenzamide-like CT reaction occurred (Figure 5). A credible analysis of the Hammett constant dependence of the CT emission energy according to eq 1 was not possible because of the limited data points and the variation of $E_{0,0}$ with the substituent (see the data shown in Figure 2 and Table 2). The apparent dependence (Figure 5), however, is higher than those of their ester counterparts **2** in which linear dependences were found with slope values lower than 0.2.⁹ In **3h–3j**, the electron acceptors (benzamide moieties) were comparable as shown with **2**,⁹ because the substituent at the amido anilino phenyl ring of **3h–3j** hardly introduced any steric effect whereas it changed the electron-withdrawing ability but not the identity of the benzamide acceptor.

To understand the reversal of the charge transfer direction, the electronic structures of the vertically (Franck–Condon, FC) excited singlet states of **3** in the gas phase were investigated by means of TDHF calculations. The calculated transition energies from the FC ground state to the FC excited state are reported in Table 3. The TDHF calculated transition energies were seen to decrease with increasing electron-withdrawing ability of the substituent at the amido anilino moiety, which is in general in agreement with the experimental observation of a red-shift in the absorption spectra (Table 2). The TDHF calculated values correspond to the (0,0) transitions and thus are at higher energies than the experimental values.^{10c} Scaling the calculated absorption maxima by a factor of 1.35 provides values that are in good

agreement with the experimental data obtained in nonpolar solvent cyclohexane, see Tables 2 and 3. It was found from Table 3 that, with only several exceptions in **3i** and **3j**, the most allowed transition indexed by the highest oscillator strength was that from the S_0 to S_1 states and corresponded mainly to the transition from HOMO to LUMO as suggested by the highest percentage value of ${}^0\chi_0$. The π -orbital characters of HOMO and LUMO, however, were found to undergo interesting variations along the **3a–3j** variations, see Scheme 3. It was seen in Scheme 3 that the π electron in the HOMO orbital of **3a** was delocalized in the whole molecule and became increasingly localized on the dimethylaminobenzoyl moiety with increasing electron-withdrawing ability of the substituent (**3b–3e**) until completely localized on the dimethylaminobenzoyl moiety (**3f–3j**). Meanwhile, the π electron in the LUMO orbital, despite delocalized but with higher density at the dimethylaminobenzoyl moiety in **3a**, became increasingly localized on the amido anilino moiety. It thus follows that upon transition from HOMO to LUMO, charge transfer occurs from the amido anilino moiety to the the dimethylaminobenzoyl moiety with **3a** and gradually changes to that from dimethylaminobenzoyl to the amido anilino moiety with, for example, **3f–3j**. The turn in the CT direction occurs around **3f** and **3g** (Scheme 3). This is in good agreement with the observations made in the substituent dependence of the CT emission. It thus appears from the calculations that an important reason for the CT direction reversal is the thermo-

dynamics of the CT process. This is also in agreement with the experimental observations made in nonpolar to moderately polar solvents (CHX, DEE, and THF) in which the CT reaction identity remained unchanged. In a highly polar solvent such as ACN, the kinetic factor seems to start to contribute to govern the CT process, Figure 5.

p-Dimethylaminobenzanilides (**3**) would thus stand as an alternative framework for designing D–A–D “balance”-like fluorescence chemosensors.^{26,27} Indeed, the total fluorescence quantum yield and the CT to LE intensity ratio of **3**, in addition to the CT emission wavelength (Figure 5), underwent a similar switch along with the substituent variations (Figure 6), which could be of use in designing **3**-based sensors based on electron donating/accepting ability variations. In this regard, it is important to point out that *p*-dimethylaminobenzanilides are dual fluorescent with strong LE emission in both CT reactions, which could be seen from a comparison of parts a and b of Figure 6. With benzanilides, however, it is known that the LE emission is very weak, and that even up to now doubt still exists that it is due to impurity or photoproducts.^{10–15} It is also worth noting in Figure 6b that the quantum yields in nonpolar solvent CHX are lower than those in polar solvents, and at the lower σ range when the benzanilide-like CT occurs, the total quantum yield increases with increasing σ . This is an indication that the (n, π^*) transition is one of the nonradiative deactivation channels of the benzanilide derivatives.^{8,10}

4. Conclusions

The intramolecular charge-transfer dual fluorescence of *p*-dimethylaminobenzanilides (**3**) in a variety of solvents was investigated. Compound **3** represent a nice combination of *p*-dimethylaminobenzamide (**1**) and benzanilide (**4**) that emit dual fluorescence but with charge-transfer reactions of different direction. The ¹H NMR chemical shift of the amido –NH proton was found to shift linearly to downfield with increasing substituent constant, and ab initio calculations indicated that the para or meta substitution at the amido anilino moiety did not result in an obvious change in the ground-state structure of *p*-dimethylaminobenzanilides (**3**). This points to the comparable variation of the amido moiety in **3** by the substitution. With **3**, the substituent dependence in the dual fluorescence in a variety of solvents, however, clearly indicated that the charge-transfer direction was reversed by substituent variation, which was found in the plots of the CT emission energy against the Hammett substituent constant that showed a turn at a σ of +0.39. In **2**, the ester counterparts of **3**, and in **4**, the derivatives of **3** without dimethylamino group, a single linear correlation was found along with similar substituent variation. It was concluded that the CT direction in *p*-dimethylaminobenzanilides (**3**) was from the amido anilino moiety to the dimethylaminobenzoyl moiety (the benzanilide-like) when the amido anilino substituent had lower σ , whereas with a substituent of higher σ , the CT in **3** turned out to be *p*-dimethylaminobenzamide-like from the dimethylamino electron donor. Ab initio calculations supported this conclusion. Therefore, the substituent effect served as an alternative method in judging the charge-transfer direction in case that multiple charge-transfer possibilities exist.

In the lower σ range, the substituent constant dependence of the CT emission energy of **3** in CHX, DEE, and THF was found to be similar to that of **4** in CHX, indicating that in nonpolar to moderately polar solvents the benzanilide-like CT reaction in **3** was not mixed by the other CT reaction. In a highly polar solvent, the benzanilide-like CT reaction was shown to be mixed by the other CT reaction. In the case when the *p*-dimethylami-

nobenzamide-like CT reaction occurred, the substituent constant dependence of the CT emission energy of **3** was found, as expected, to be higher than that in their ester counterparts **2**.⁹ The observation that with the majority of **3** the charge transfer is in the opposite direction to that in **1**, even when the amido anilino phenyl ring in **3** is substituted by an electron withdrawing substituent, points to the difference of aniline as an electron donor against alkylamine that aniline is actually a much stronger electron donor. This would be of use in designing electron donor/acceptor substituted CT sensing systems.

p-Dimethylaminobenzanilides are dual fluorescent, and the CT emission wavelength, the total fluorescence quantum yield, and the CT to LE emission intensity ratio undergo interesting variations when the amido anilino substituent is varied, which indicates that the **3**-based dual fluorescent chemosensors could be constructed. The CT direction reversal behavior in **3** suggests that it could be an alternative framework for constructing D–A–D’ balance-like fluorescence sensors.^{26,27}

Acknowledgment. We thank the National Natural Science Foundation of China (Grant Nos. 29975023 and 20175020), the Ministry of Education (MOE) of China, and the Natural Science Foundation of Fujian Province for support of this work. The Varian Cary 300 UV–vis absorption spectrophotometer was purchased under the support of the German Volkswagenstiftung (Grant No. I/77 072).

References and Notes

- Grabowski, Z. R.; Rotkiewicz, K.; Siemiarz, A.; Cowley, D. J.; Baumann, W. *Nouv. J. Chim.* **1979**, *3*, 443.
- Rettig, W. *Angew. Chem., Int. Ed. Engl.* **1986**, *25*, 971.
- Zachariasse, K. A.; von der Haar, T.; Hebecker, A.; Leinhos, U.; Kühnle, W. *Pure Appl. Chem.* **1993**, *65*, 1745.
- Schuddeboom, W.; Jonker, S. A.; Warman, J. M.; Leinhos, U.; Kühnle, W.; Zachariasse, K. A. *J. Phys. Chem.* **1992**, *96*, 10809.
- Il’chev, Y.; Kühnle, W.; Zachariasse, K. A. *J. Phys. Chem. A* **1998**, *102*, 5670.
- Rettig, W.; Zietz, B. *Chem. Phys. Lett.* **2000**, *317*, 187.
- Dobkowski, J.; Wójcik, J.; Koźmiński, W.; Kolos, R.; Waluk, J.; Michl, J. *J. Am. Chem. Soc.*, **2002**, *124*, 2406.
- Braun, D.; Rettig, W.; Delmond, S.; Létard, J.-F.; Lapouyade, R. *J. Phys. Chem. A* **1997**, *101*, 6836.
- Huang, W.; Zhang, X.; Ma, L.-H.; Wang, C.-J.; Jiang, Y.-B. *Chem. Phys. Lett.* **2002**, *352*, 401.
- (a) Lewis, F. D.; Long, T. M. *J. Phys. Chem. A* **1998**, *102*, 5327. (b) Lewis, F. D.; Liu, W. Z. *J. Phys. Chem. A* **1999**, *103*, 9678. (c) Lewis, F. D.; Liu, W. Z. *J. Phys. Chem. A* **2002**, *106*, 1976.
- (a) Tang, G.-Q.; MacInnis, J.; Kasha, M. *J. Am. Chem. Soc.* **1987**, *109*, 2531. (b) Heldt, J.; Gormin, D.; Kasha, M. *J. Am. Chem. Soc.* **1988**, *110*, 8255. (c) Heldt, J.; Gormin, D.; Kasha, M. *Chem. Phys. Lett.* **1988**, *150*, 433. (d) Heldt, J.; Gormin, D.; Kasha, M. *Chem. Phys.* **1989**, *136*, 321.
- Azumaya, I.; Kagechika, H.; Fujiwara, Y.; Itoh, M.; Yamaguchi, K.; Shudo, K. *J. Am. Chem. Soc.* **1991**, *113*, 2833.
- (a) Heldt, J.; Heldt, J. R.; Szatan, E. J. *J. Photochem. Photobiol. A: Chem.* **1999**, *121*, 91. (b) Brozis, M.; Heldt, J.; Heldt, J. R. *J. Photochem. Photobiol. A: Chem.* **1999**, *128*, 39.
- (a) Lucht, S.; Stumpe, J.; Rutloh, M. *J. Fluorescence* **1998**, *8*, 153. (b) Lucht, S.; Stumpe, J. *J. Lumin.* **2000**, *91*, 203.
- (a) Zhang, X.; Sun, X.-Y.; Wang, C.-J.; Jiang, Y.-B. *J. Phys. Chem. A* **2002**, *106*, 5577. (b) Zhang, X.; Ma, L.-H.; Sun, X.-Y.; Wang, C.-J.; Wu, F.-Y.; Li, Z.; Jiang, Y.-B. *Chem. J. Chin. University* **2002**, *23*, 1701.
- Malval, J.-P.; Lapouyade, R. *Helv. Chim. Acta* **2001**, *84*, 2439.
- (a) Jacques, P.; Allonas, X.; Dossot, M. *J. Photochem. Photobiol., A: Chem.* **2001**, *142*, 91. (b) Jacques, P.; Allonas, X. *Chem. Phys. Lett.* **1995**, *233*, 533.
- Demas, J. N.; Crobys, G. A. *J. Phys. Chem.* **1971**, *75*, 991.
- (a) Frisch, M. J.; Trucks, G. W.; Schlegel, H. B.; Scuseria, G. E.; Robb, M. A.; Cheeseman, J. R.; Zakrzewski, V. G.; Montgomery, J. A., Jr.; Stratmann, R. E.; Burant, J. C.; Dapprich, S.; Millam, J. M.; Daniels, A. D.; Kudin, K. N.; Strain, M. C.; Farkas, O.; Tomasi, J.; Barone, V.;

Cossi, M.; Cammi, R.; Mennucci, B.; Pomelli, C.; Adamo, C.; Clifford, S.; Ochterski, J.; Petersson, G. A.; Ayala, P. Y.; Cui, Q.; Morokuma, K.; Malick, D. K.; Rabuck, A. D.; Raghavachari, K.; Foresman, J. B.; Cioslowski, J.; Ortiz, J. V.; Stefanov, B. B.; Liu, G.; Liashenko, A.; Piskorz, P.; Komaromi, I.; Gomperts, R.; Martin, R. L.; Fox, D. J.; Keith, T.; Al-Laham, M. A.; Peng, C. Y.; Nanayakkara, A.; Gonzalez, C.; Challacombe, M.; Gill, P. M. W.; Johnson, B. G.; Chen, W.; Wong, M. W.; Andres, J. L.; Head-Gordon, M.; Replogle, E. S.; Pople, J. A. *Gaussian 98*; Gaussian, Inc.: Pittsburgh, PA, 1998.

(20) Jiang, Y.-B. *J. Photochem. Photobiol. A: Chem.* **1994**, *78*, 125.

(21) Hansch, C.; Leo, A.; Taft, R. W. *Chem. Rev.* **1997**, *91*, 1165.

(22) Demeter, A.; Bérces, T.; Zachariasse, K. A. *J. Phys. Chem. A* **2001**, *105*, 4611.

(23) Kapelle, S.; Rettig, W.; Lapouyade, R. *Chem. Phys. Lett.* **2001**, *348*, 416.

(24) Yang, J.-S.; Chiou, S.-Y.; Liao, K.-L. *J. Am. Chem. Soc.* **2002**, *124*, 2518.

(25) For details of MOLDEN, the reader is directed to <http://www.cmbi.kun.nl/~schaff/molden/molden.html>.

(26) Crochet, P.; Malval, J.-P.; Lapouyade, R. *Chem. Commun.* **2000**, 289.

(27) Rurack, K.; Rettig, W.; Resch-Genger, U. *Chem. Commun.* **2000**, 407.